GENERAL PHYSICS

I. RADIO ASTRONOMY*

Academic and Research Staff

Prof. A. H. Barrett
Prof. B. F. Burke
Prof. R. M. Price
Prof. D. H. Staelin
Dr. G. D. Papadopoulos
J. W. Barrett
D. C. Papa

Graduate Students

R. H. Cohen
P. C. Crane
M. S. Ewing
T. D. Halket
H. F. Hinteregger
P. L. Kebabian
C. A. Knight
K-S. Lam
K-Y. Lo
P. C. Myers
P. W. Rosenkranz
P. R. Schwartz
J. H. Spencer
J. W. Waters
A. R. Whitney

A. STELLAR INTERFEROMETER

The fringes formed in the stellar interferometer will be detected by photomultiplier tubes operating in the pulse counting mode, as noted in a previous report.[1] The signals to be detected, both for guidance and for fringe measurement, are the difference in the output pulse rates of a pair of phototubes. The pulses from each of the six pairs of phototubes that will be used are first synchronized to a 4-MHz clock pulse train, and then counted by 10-bit bi-directional counters. Every 100 μs the contents of these counters are loaded into 10-bit shift registers for serial readout, and the counters are reset.

The guidance channels do not need to operate at high input pulse rates, and therefore the synchronizers used with them can be single-stage synchronizers; that is, the maximum output pulse rate is half the clock rate. In order to get better linearity at high counting rates, the counters in the fringe channels have two stages, and have a maximum output rate equal to the clock rate.

Simple formulas can be derived for the counting loss of the two kinds of synchronizer as a function of the input pulse rate, provided that the input pulse train is accurately modeled as a Poisson process. In reality, the pulses from the photomultiplier assemblies have significant width and dead times, and thus the formulas will provide only a rough guide to the counting loss. Since an accurate theoretical derivation would be quite complicated, and only tangential to the purposes of this research, the simplest solution is to measure the counting loss experimentally.

The basic word length of the processing circuitry is 25 bits, so the shift registers are read out in bursts of 10 bits, followed by 15 sign bits. The shift registers of the guidance counters are read out in series, as are those of the fringe signal counters. The bit rate is 1 MHz in both cases, the remaining 50 bits in the fringe

*This work was supported in part by California Institute of Technology Contract 952568, and in part by the Sloan Fund for Basic Research (M.I.T. Grant 241).

signal channel being blanks, and usable if other fringe signal channels are added later. This format is used because both fringe signals are processed identically, as are the four guidance signals, and thus the processor can be constructed to use dual 100-bit MOS shift registers, which are readily available at low cost, for its memory.

Each bi-directional counter measures the difference in the number of pulses from the two phototubes connected to it. For the fringe-detecting phototubes, counters have also been provided to measure the sum of the pulses from the two tubes. This sum is needed in order to normalize the detected and integrated fringe signal to the total light received. These counters are also read out and reset at 10 kHz. If we wished to do so, little extra work would be required to use the outputs of these counters to study the statistics and power spectrum of stellar scintillation. Although there are already many published measurements of these quantities, such measurements might be of interest when taken together with the measurements of angular and phase fluctuations, that form one of the basic goals of this project.

Because of the presence of scintillation, the light in the fringe channel is to be chopped at 5 kHz, and the 5-kHz fringe signal is then detected by synchronously reversing the inputs to the bi-directional counters. This is done during the 1 μsec of each cycle when the counting is inhibited and the counters are being read out. The result is that the power spectrum of the output of the bi-directional counters is shown in Fig. I-1.

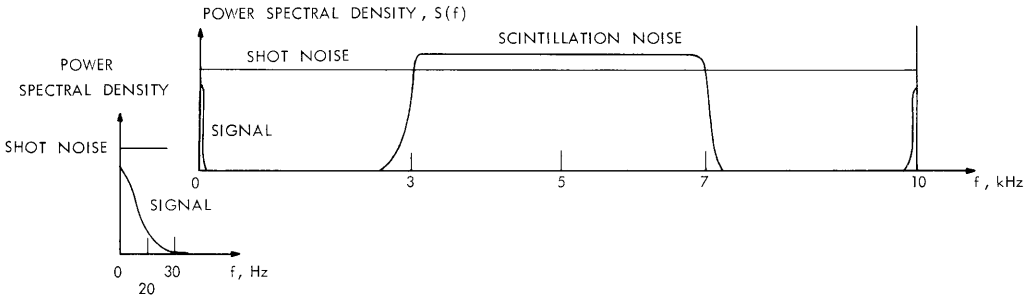

Fig. I-1. Power spectrum of the output from the bi-directional counters in the fringe channel.

In order to have the data available for later processing, in particular for spectral analysis, the signal must be recorded on magnetic tape. Because of the lowpass nature of the signal, an appropriate sampling rate is 10 kHz/128, = 78 1/8 Hz. Any higher sampling rate would only record more noise, with negligible increase in the recorded signal. Furthermore, an approximately matched filter, followed by a squarer and integrator, must be available during the observations, so that the observer can adjust the path length and be sure that the fringes are in the field of

view. Thus we are faced with the problem of filtering the spectrum in Fig. I-1 so that the word rate can be reduced by a factor of 128 without aliasing too much noise into the signal band.

Based on the brightness of the stars to be observed and the power spectrum of stellar scintillation, we find that an appropriate frequency response for the filter is $H(f) \sim \left(\frac{f}{78\ 1/8}\right)^{-2}$ beyond the passband. Since the signal will later be subjected to matched filtering, a flat passband is not required.

A particularly convenient and economical way of building such a filter will be described. It is called a "duplicating" filter, and the reason for the name will soon be evident. The filter structure will be derived first intuitively, and then more formally.

1. Duplicating Filters

Eadem Mutata Resurgo ..... Jacob Bernoulli

Observe that since the only purpose of the filter is to reduce the word rate without unduly increasing the noise level in the signal band that is due to aliasing, the signal may be passed through a filter with a frequency response like that sketched in Fig. I-2a, followed by a sampler operating at half the incoming word rate.

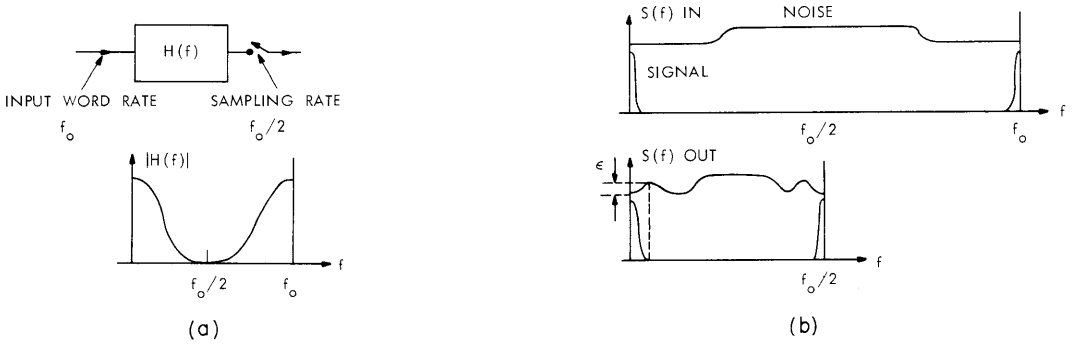

Fig. I-2. (a) A unit cell of the filter. (b) Input and output spectra.

As sketched in Fig. I-2b, the power spectrum of the output is not greatly different in shape from that of the input, and the word rate has been reduced by a factor of two. The increase in the noise level in the passband, ϵ, caused by aliasing of scintillation noise, can be made arbitrarily small by having a high enough order zero at $H(f_o/2)$. The output of the filter and sampler is now fed into another, which is structurally identical to the first but operating at 1/2 the initial word rate, then into another working at 1/4 the initial rate, and so forth. Eventually, the sampling rate is reduced to

the Nyquist sampling rate of the signal, and the process must stop. Actually, the addition of further stages must be stopped somewhat before this because the filter that is to be used does not cut off sharply, and therefore the region of low transmission will no longer prevent aliasing of noise into the outer parts of the signal band.

A class of filters of particular interest is the boxcar integrator, and filters obtained by cascading boxcar integrators. These can be very simply and economically built by using shift registers, adders, and subtractors. Separate multipliers and stored coefficients are not required – the structure of a cascade of boxcar integrators inherently generates the required multiplications.

If we consider the problem of aliasing of noise into the signal band, it turns out that a single boxcar integrator will not work in the present case, but that two boxcars in cascade are satisfactory. The time-domain terminology of this filter is illustrated in Fig. I-3, where h_n is the digital analog of the impulse response, that is, the output at word n caused by the word w_o having value 1. [Note that h_n is also the response of word w_o caused by word w_{-n} having the value 1. This is the sense in which the impulse response of a sampled system should be considered.] The time origin is taken to coincide with the operation of the sampler, and in a cascaded system, it coincides with the operation of the lowest frequency sampler.

We see that

$$\begin{aligned} y_o &= w_o + 2w_{-1} + w_{-2} \\ y_1 &= w_2 + 2w_1 + w_o \\ y_2 &= w_4 + 2w_3 + w_2 \\ &\text{etc.} \end{aligned} \tag{1}$$

Let the y_n be used as the input to another unit cell, identical to the one above, and having an output z_n.

$$\begin{aligned} z_1 = y_2 + 2y_1 + y_o &= w_4 + 2w_3 + w_2 \\ &\quad + 2 \cdot (w_2 + 2w_1 + w_o) \\ &\quad + w_o + 2w_{-1} + w_{-2} \\ &= w_4 + 2w_3 + 3w_2 + 4w_1 + 3w_o + 2w_{-1} + w_{-2} \\ z_2 = y_4 + 2y_3 + y_2 &= w_8 + 2w_7 + 3w_6 + 4w_5 + 3w_4 + 2w_3 + w_2 \\ &\text{etc.} \end{aligned} \tag{2}$$

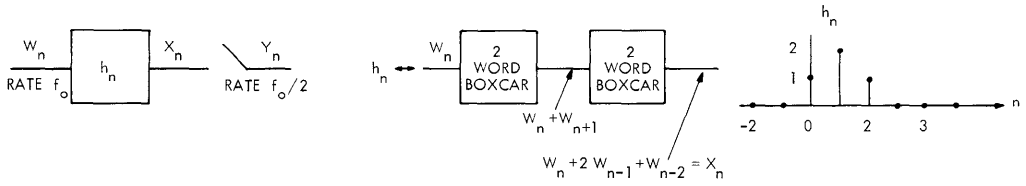

Fig. I-3. Unit cell made from two 2-word boxcar integrators, in the time domain.

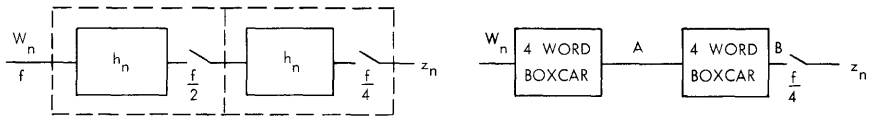

Fig. I-4. Two cascaded unit cells, and their duplicate.

Now, compare the cascaded system described above with one constructed as shown in Fig. I-4.

At point A, the signal is $w_n+w_{n-1}+w_{n-2}+w_{n-3}$.

At point B, the signal is

$$\begin{aligned} & w_n+w_{n-1}+w_{n-2}+w_{n-3} \\ + \quad & w_{n-1}+w_{n-2}+w_{n-3}+w_{n-4} \\ + \quad & w_{n-2}+w_{n-3}+w_{n-4}+w_{n-5} \\ + \quad & w_{n-3}+w_{n-4}+w_{n-5}+w_{n-6} \\ = \quad & w_n+2w_{n-1}+3w_{n-2}+4w_{n-3}+3w_{n-4}+2w_{n-5}+w_{n-6}. \end{aligned} \tag{3}$$

Thus, the two systems have exactly the same transfer function. Moreover, the new system has exactly the same structure as the cascaded system's unit cell, differing only in that the boxcar integrators are longer by a factor of 2, as is the sampling period. It may readily be verified that as more unit cells are added to the cascaded system, the response continues to be the same as that of the duplicate system formed by lengthening the boxcar integrators and sampling period of the unit cell.

At this point, observe that the duplicating property is associated with the structure used to realize h_n, and not with h_n itself. In other words, the duplicate system mentioned above might have been built with a structure completely different from that of the unit cell. The important thing is that when the structure of the unit cell is duplicated, the response is the same as the response of the cascaded system.

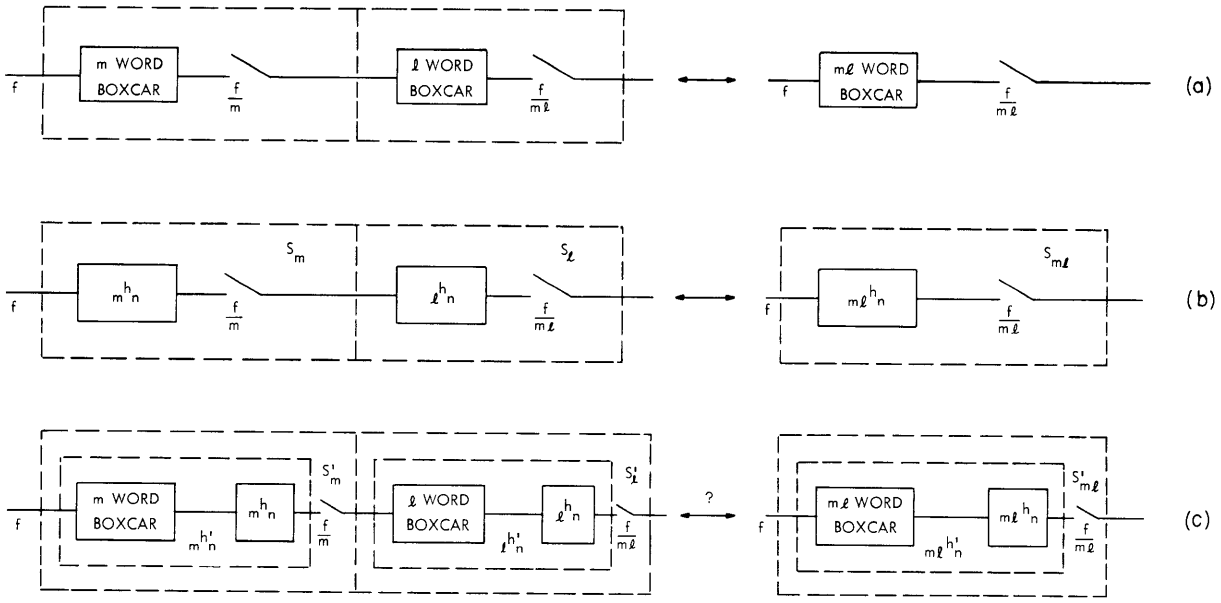

Fig. I-5. Filters used in deriving the filter structure of Fig. I-8.

In the example above, a cascade of two boxcars was used. Figure I-5a shows the simpler case of a filter with unit cells containing a single boxcar, and the duplicate filter with the same response. In Fig. I-5b there is a more general pair of unit cells, S_m and S_ℓ, and it is given that the third filter, $S_{m\ell}$, has the same response as S_m cascaded with S_ℓ. This means that the impulse responses are related by

$$
\begin{array}{l}
{}_{\ell}h_0\cdot({}_{m}h_0 \quad {}_{m}h_1 \quad {}_{m}h_2 \cdots {}_{m}h_m \quad {}_{m}h_{m+1} \cdots) \\
+{}_{\ell}h_1\cdot(\qquad\qquad\qquad\qquad {}_{m}h_0 \quad {}_{m}h_1 \cdots\cdots) \\
\quad \vdots \\
\hline
={}_{\ell}h_0\cdot{}_{m}h_0 \quad {}_{\ell}h_0\cdot{}_{m}h_1 \cdots\cdots ({}_{\ell}h_0\cdot{}_{m}h_m+{}_{\ell}h_1\cdot{}_{m}h_0)\cdots\cdots \\
= \; {}_{m\ell}h_0 \quad {}_{m\ell}h_1 \cdots\cdots {}_{m\ell}h_m \cdots\cdots
\end{array}
\tag{4}
$$

Thus

$$
{}_{m\ell}h_k = \sum_{j=0}^{k} {}_{\ell}h_j\cdot{}_{m}h_{k-mj}\cdot \tag{5}
$$

Note that all impulse response coefficients h_n must be 0 for $n < 0$, since the system must obey causality. Also, note that there is no requirement that S_m, S_ℓ, and $S_{m\ell}$ be duplicate structures, but that Fig. I-5a shows one case in which they are duplicates.

In Fig. I-5c, a boxcar has been added to the filters contained in S_m, S_ℓ, and $S_{m\ell}$. The new impulse responses are

$$ {}_m h'_n = \sum_{q=0}^{m-1} {}_m h_{n-q} \tag{6} $$

$$ {}_\ell h'_n = \sum_{r=0}^{\ell-1} h_{n-r} \tag{7} $$

$$ {}_{m\ell} h'_n = \sum_{s=0}^{m\ell-1} {}_{m\ell} h_{n-s} = \sum_{s=0}^{m\ell-1} \sum_{j=0}^{n-s} {}_\ell h_j \cdot {}_m h_{n-s-mj} \tag{8} $$

$$ = \sum_{s=0}^{m\ell-1} \sum_{j=0}^{[(n-s)/m]} {}_\ell h_j \cdot {}_m h_{n-s-mj}. \tag{9} $$

where $[(n-s)/m]$ denotes the maximum positive integer in $(n-s)/m$.

By analogy with Eq. 5, the impulse response of the cascade of S'_m and S'_ℓ is

$$ {}_{m\ell} h''_n = \sum_{j=0}^{n} {}_\ell h'_j \cdot {}_m h'_{n-mj} = \sum_{j=0}^{n} \left(\sum_{r=0}^{\ell-1} {}_\ell h_{j-r} \right) \left(\sum_{q=0}^{m-1} {}_m h_{n-mj-q} \right) = \sum_{j=0}^{n} a_j. \tag{10} $$

$$ = \sum_{r=0}^{\ell-1} \sum_{q=0}^{m-1} \sum_{j=0}^{n} {}_\ell h_{j-r} \cdot {}_m h_{n-mj-q} = \sum_{r=0}^{\ell-1} \sum_{q=0}^{m-1} b_{rq}. \tag{11} $$

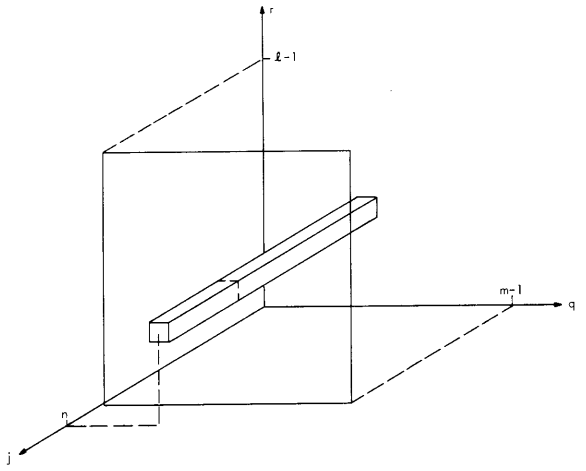

Fig. I-6.

Geometrical interpretation of Eqs. 10 and 11. The summation a_j is over points in a plane parallel to the rq plane. The summation b_{rq} is over the points in a column parallel to the j axis.

Figure I-6 illustrates the meaning of the summations in Eqs. 10 and 11.

Since $h_{n<0} = 0$,

$$b_{rq} = \sum_{j=0}^{n} \ell^{h}_{j-r} \cdot m^{h}_{n-q-mj} = \sum_{(j-r)=0}^{n-r} \ell^{h}_{(j-r)} \cdot m^{h}_{n-(q+mr)-m(j-r)}$$

$$= \sum_{J=0}^{n-r} \ell^{h}_{J} \cdot m^{h}_{n-S-mJ}, \tag{12}$$

where $J = j - r$ and $S = q + mr$.

The only cases of interest are $m \geq 2$, and $q \geq 0$. Therefore, $S > r$ and $n - r > n - S$. All of the terms in (12) with $J > [(n-S)/m]$ are 0; therefore,

$$b_{rq} = \sum_{J=0}^{[(n-S)/m]} \ell^{h}_{J} \cdot m^{h}_{n-S-mJ} \tag{13}$$

$$m\ell^{h''}_{n} = \sum_{r=0}^{\ell-1} \sum_{q=0}^{m-1} \sum_{J=0}^{[(n-S)/m]} \ell^{h}_{J} \; m^{h}_{n-S-mJ} \tag{14}$$

Figure I-7 illustrates how the first two summations of Eq. 14 are replaced by

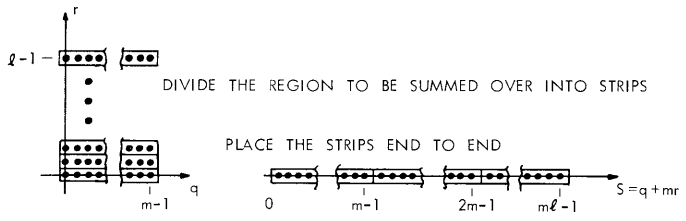

Fig. I-7. Geometrical interpretation of the variable S.

a single summation, so that

$$m\ell^{h''}_{n} = \sum_{S=0}^{m\ell-1} \sum_{J=0}^{[(n-S)/m]} \ell^{h}_{J} \; m^{h}_{n-S-mJ} \equiv m\ell^{h'}_{n}. \tag{15}$$

Since the boxcar integrators of Fig. I-5a will work for the primitive structures S_m, S_ℓ, and $S_{m\ell}$, it follows by induction that any structure of the kind

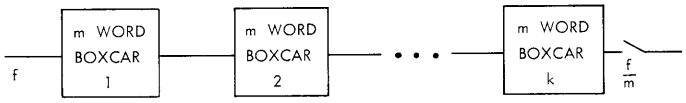

Fig. I-8. The general unit cell of a duplicating filter.

shown in Fig. I-8 is the unit cell of a duplicating filter.

Duplicating filters evidently form a very small subset of the filters obtainable by the method illustrated in Fig. I-2. For example, the unit cells at the end of the cascade might have k larger than those at the beginning, in order to allow the word rate to be reduced closer to the Nyquist sampling rate of the signal without aliasing too much noise into the signal band, but the over-all response would not duplicate that of the unit cell, simply because there are two or more different kinds of unit cell. Why, then, are duplicating filters of particular interest?

The most important reason is that duplicating filters, like all filters realized by the method in Fig. I-2, remove unwanted parts of the spectrum by binary elimination. Thus, to filter a signal and reduce its word rate by 2^n, the required memory varies as n instead of 2^n, as it would if the filter were realized directly. Word rate reduction by $\prod_{j=1}^{n} m_j$ is possible also, the case of all $m_j = 2$ being the most economical.

The duplicating filter is an especially systematic way of doing this. Whenever a frequency response of the form $\left(\frac{\sin 2^n \pi f/f_o}{\sin \pi f/f_o}\right)^k$ will provide the required filtering, the filter and sampler are realized by n identical unit cells, each made from k two-word boxcars.

In the real world, there are many situations wherein a signal must be lowpass-filtered and sampled at far below the original word rate, but the exact shape of the frequency response and the exact reduction in the word rate are not very important, as long as not too much noise is aliased into the signal band. This is often the case in geophysical applications, for instance. Duplicating filters are suitable for these purposes.

Another advantage of duplicating filters, although not unique to them, is that their impulse responses have finite duration and integer coefficients. Therefore, it is often possible to accept the growth in the word length by one bit for each two-word boxcar, and in that way get a filter completely free of truncation or rounding noise.

A very important advantage of duplicating filters is that they are realized by a cascade of identical unit cells, and these can be built with simple and economical circuitry.

Finally, duplicating filters are of interest in themselves because of the duplicating property. One very interesting question is, What other structures, if any, have a duplicating property similar to that of the structure given above? Another area for study is the general properties of filters obtained by the method in Fig. I-2.

Duplicating filters are built from boxcar integrators, and these are built from shift registers, adders, and subtractors. Some of the ways of obtaining a boxcar integrator are shown in Fig. I-9. For m = 2 and m = 3, Fig. I-9a uses fewer parts, and for m > 3, Fig. I-9b is better. In Fig. I-9c, the method of combining the final boxcar integrator and sampler of a unit cell is shown.

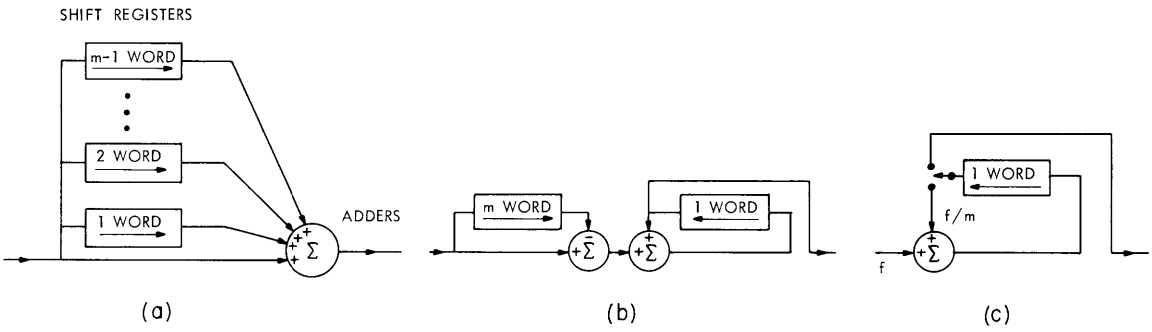

Fig. I-9. Realizations of boxcar integrators using shift registers and adders.

When a large number of boxcar integrators are cascaded, it is often important to prevent the delays associated with the adders from accumulating, since the shift registers will usually be MOS units, operated synchronously from a common clock source. For this reason, the output in Fig. I-9b is taken from the shift register rather than from the adder. The additional one-word delay is of no practical importance.

Note that when a duplicating filter reduces the word rate, the bit rate remains the same, and thus the later stages of a duplicating filter are quiescent most of the time. When a unit cell is operating its power consumption is P_r, and when it is quiescent it uses P_q. For word-rate reductions of $2^n \gg 1$, the total power used is $\sim nP_q + 2(P_r - P_q)$. If dynamic shift registers are used, the stored words will generally have to be recirculated during the quiescent phase, and $P_q = P_r$. If static shift registers are used, the clock signal can be stopped during the quiescent phase, although P_q is still relatively high. If a low-power logic type such as complementary MOS is used, or n the word rate is high enough that dynamic shift registers can be used without recirculating (and complementary MOS used for the rest of the circuits in the unit cell), then the power consumption can be very small, which might be an important advantage in some cases, such as geophysical instrumentation.

For the important case of m = 2, and where the word rate is not too high, it is possible to take advantage of the availability of very long shift registers at low cost per bit, in order to obtain a large value of k. A circuit to do this is shown in Fig. I-10. A typical situation in which this would be advantageous is k = 8, word length = 32 bits, so that the large register is 256 bits.

In all of these, several data streams may be processed identically by multiplexing the words serially, lengthening the shift registers, and resetting the carry flip-flops of the adders at the beginning of each word.

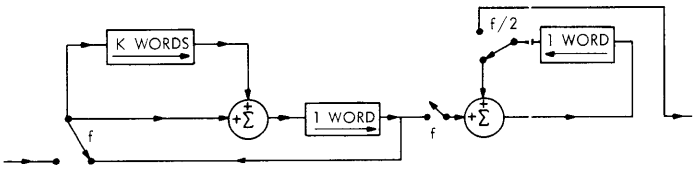

Fig. I-10.
Unit cell with most of the memory in a single shift register.

Finally, the duplicating filter structure may be realized by using a general-purpose digital computer. Obviously, it would be wasteful to use the computer to realize a real-time duplicating filter. For off-line filtering and sampling, the input data are read in as a block of $k2^n$ words, and the programmer now has the choice of filtering this with a duplicating filter, or directly forming a weighted sum of the input points. The first stage of the duplicating filter is computed with $k^2 \times 2^n$ additions, the second stage with $k^2 \times 2^{n-1}$, etc., for a total of $\sim 2k^2 \times 2^n$ additions. The direct method requires $k2^n$ multiplications and additions, so that the faster filtering method will depend, for the most part, on the ratio of add time to multiply time. For a very small machine, the multiply operation must be programmed, in which case the duplicating filter would often be faster, besides not requiring a table of coefficients. For a very large computer with multiplication a permanently wired part of the central processor, the direct method would be faster.

P. L. Kebabian

References

1. P. L. Kebabian, "Optical Stellar Interferometer," Quarterly Progress Report No. 100, Research Laboratory of Electronics, M.I.T., January 15, 1971, pp. 44-45.

B. TRANSMISSION OF CARBON DIOXIDE: Q BRANCH

The Q-branch transmission of the 15 μ carbon dioxide absorption band is important for sensing the atmospheric temperature profile. Evaluation of the transmission by integrating point by point on the spectrum is time-consuming, while no band model has been devised that satisfactorily represents the intense line distribution. An

efficient computational procedure is given in this report which improves the accuracy and ease of computation of expressions suggested by Yamamoto and Aida.[1]

In a particular vibrational band, a spectral line is centered at the frequency

$$\omega_J = \omega_o + BJ(J+1), \tag{1}$$

where

ω_o = band origin of the vibrational transition

B = difference in rotation constants of the upper and lower energy states

J = rotational number of the lower energy state.

Adjacent lines are separated by

$$b_J = \frac{1}{2}\left[(\omega_{J+\Delta J} - \omega_J) + (\omega_J - \omega_{J-\Delta J})\right]$$

$$= B(2J+1)\,\Delta J, \tag{2}$$

where $\Delta J = 1$ or 2 according to selection rules.

The line has integrated intensity

$$S_J = S_o |A_J|^2 \exp[-\mu J(J+1)], \tag{3}$$

where

S_o = total integrated intensity of the vibrational band

μ = (hc/kT) × (rotation constant of the lower energy state)

h = Planck's constant

k = Boltzmann's constant

T = absolute temperature of the gas

$|A_J|^2$ = rotational matrix element, rapidly approaching 2J+1 for large J.

Under the assumption that the Lorentz line shape is of half-width a, the absorption coefficient at a particular frequency ω is

$$k_Q(\omega) = \frac{1}{\pi} \sum_J S_J \frac{a}{a^2 + (\omega - \omega_J)^2}, \tag{4}$$

where summation is over all allowed J, typically 2-80 by 2 before S_J becomes negligible.

By substituting $t = \mu J(J+1)$ and allowing $J = 2, 4, 6, \ldots$, the summation in Eq. 4 transforms to the integral

$$k_s(\omega) = \frac{S_o y^2}{2\pi a \mu} \int_0^\infty \frac{e^{-t}}{y^2 + (t+x)^2}\, dt, \tag{5}$$

where

$$x = -\frac{\mu}{B}(\omega - \omega_o)$$

$$y = \mu a / B.$$

The integral (5) has been analytically evaluated by Yamamoto and Aida.[1]

$$k_s(\omega) = -\frac{S_o y}{2\pi a \mu}\, e^x [\sin y\, \mathrm{Re}\, E_1(z) + \cos y\, \mathrm{Im}\, E_1(z)], \tag{6}$$

where

$$E_1(z = x+iy) = \int_1^\infty \frac{e^{-z\zeta}}{\zeta}\, d\zeta \tag{7}$$

The exponential integral (7) for complex arguments has application to other research areas. For atmospheric transmission, the magnitude of parameters involved requires much finer step size than that with which $E_1(z)$ has been tabulated.[2] These equations are more applicable and easily implemented on a computer:

$$\mathrm{Re}\, E_1(z) = E_1(x) + re^{-x} \sum_{m=2,4,6,\ldots} \frac{(-1)^{m/2}}{m!} r^{m-1} [x^{m-1} + (m-1)x^{m-2} + \ldots + (m-1)!]$$

$$\mathrm{Im}\, E_1(z) = p + re^{-x} \sum_{m=1,3,5,\ldots} \frac{(-1)^{\frac{m+1}{2}}}{m!} r^{m-1} [x^{m-1} + (m-1)x^{m-2} + \ldots + (m-1)!] \tag{8}$$

where

$$p = \begin{cases} 0 & x > 0 \\ -\pi & x < 0 \end{cases}$$

$$r = y/x \qquad |r| < 1$$

and $E_1(x)$ is well represented by polynomials, as in the IBM Scientific Subroutine Package. Since $|r| \ll 1$, only one or two terms are necessary in the summations. By expanding the series in terms of $1/r$, $E_1(|r|>1)$ can be similarly derived but need not be considered here.

If a spectrometer channel occupies the frequency interval ω_{out} outside a Q branch and includes lines up to $J = J'$ inside, then obviously the average transmission $\bar{\tau}$ of the whole channel for an optical mass u is the weighted sum

$$\bar{\tau} = \frac{\omega_{out} \int_{\omega_{out}} \exp[-k_s(\omega)u]\, d\omega + \sum^{J'} b_J \tau_J}{\omega_{out} + \sum^{J'} b_J} \tag{9}$$

where

$$\tau_J = \int_{b_J} \exp[-k_Q(\omega)u]\, d\omega. \tag{10}$$

The integral $\int_{\omega_{out}} \exp[-k_s(\omega)u]\, d\omega$ for frequencies outside the Q branch represents absorption by line wings only. It can be easily evaluated, since $k_s(\omega)$ is a smooth function (at all pressures). Inside the Q branch, τ_J in Eq. 10 is more difficult to evaluate, however, owing to the fine structure of spectral lines at low pressures. Mathematically, the passage of summation to integration in Eqs. 4 and 5 is valid only when $B \ll a$.

Yamamoto[1] has suggested the approximation

$$\tau_J \approx \tau_J^* \exp[-(k_s(\omega_J)-\bar{k}_J)u] \tag{11}$$

where $k_s(\omega_J)$ is given by Eq. 6, and

$$\bar{k}_J = \frac{1}{b_{J/2}} \int_0^{b_J/2} \frac{S_J}{\pi} \frac{a}{a^2 + \omega^2}\, d\omega$$

$$= \frac{2S_J}{\pi b_J} \tan^{-1}(b_J/2a) \tag{12}$$

τ_J^*, the direct contribution of one spectral line alone, is given by

$$\tau_J^* = \int_{b_J} \exp[-k_J(\omega)u]\, d\omega$$

$$= \frac{1}{b_{J/2}} \int_0^{b_J/2} \exp\left[-\frac{S_J u}{\pi a} \frac{a^2}{a^2+\omega^2}\right] d\omega$$

$$= \int_0^1 \exp\left[-\xi \frac{k^2}{k^2+p^2}\right] dp \qquad (13)$$

where

$k = 2a/b_J$

$\xi = 2x(1+k^2)$

$x = S_J u/2\pi a(1+k^2)$

$p = 2\omega/b_J$.

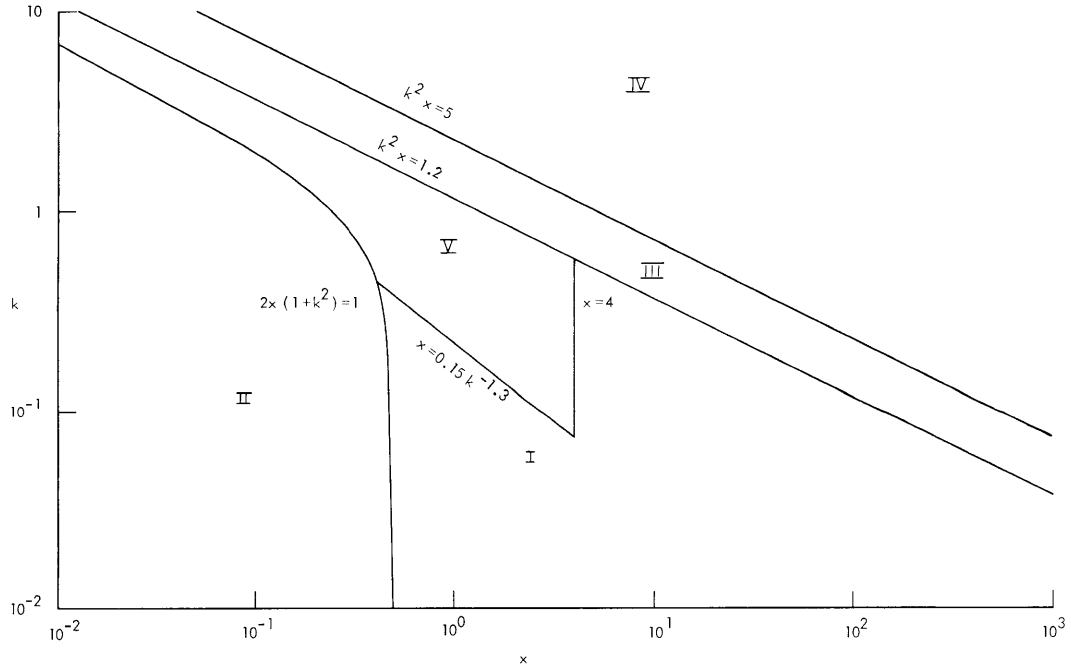

Fig. I-11. Regions of utilization to evaluate $\int_0^1 \exp\left[-2x \frac{k^2(1+k^2)}{k^2+p^2}\right] dp$. (See Eqs. 14.) Note that partition is actually good for $10^{-3} < x < 10^5$.

The integral (13) has been evaluated by Wyatt et al.[3] Better results can be calculated by using appropriate equations over different regions of x and k. With the partition in Fig. I-11, the equations applicable to different regions are as follows.

$$\text{I:}\quad \tau_J^* = e^{-\xi\epsilon^2} + 2k\xi\left[A - \frac{\pi}{4}e^{-\xi/2}\left(I_o\left(\frac{\xi}{2}\right) + I_1\left(\frac{\xi}{2}\right)\right)\right] - \frac{1}{2}k\left[A - \epsilon\, e^{-\xi\epsilon^2}\right];\ A = \frac{1}{2}\sqrt{\frac{\pi}{\xi}}\,\mathrm{erf}\left[\epsilon\sqrt{\xi}\right]$$

$$\text{II:}\quad \tau_J^* = 1 - k\sum_{n=0}^{3}(-1)^n\frac{\xi^{n+1}}{(n+1)!}F_n;\ F_n = \frac{k^{2n-1}}{2n(1+k^2)^n} + \frac{2n-1}{2n}F_{n-1}$$

$$F_o = \tan^{-1}(1/k)$$

$$\text{III:}\quad \tau_J^* = \sum_{n=0}^{N}\exp\left[-\xi\frac{k^2}{k^2 + (n\Delta)^2}\right];\ \Delta = \frac{1}{N}$$

$$N \approx 20$$

$$\text{IV:}\quad \tau_J^* = 0$$

$$\text{V:}\quad \tau_J^* = e^{-\xi\epsilon^2} - \frac{k\xi}{2}e^{-\xi/2}\left[I_o\left(\frac{\xi}{2}\right) + I_1\left(\frac{\xi}{2}\right)\right](\pi-\psi) + k\,e^{-\xi/2}\sum_{n=1}^{6}\left[2I_n\left(\frac{\xi}{2}\right) + \frac{\xi}{n}\left(I_n\left(\frac{\xi}{2}\right) + I_{n+1}\left(\frac{\xi}{2}\right)\right)\right]\sin n\psi, \qquad (14)$$

where

$$\epsilon = k/\sqrt{1 + k^2}$$

$$\psi = 2\tan^{-1} k$$

I_n = modified Bessel function of order n.

The relative error is generally better than 0.2% transmittance except in regions III

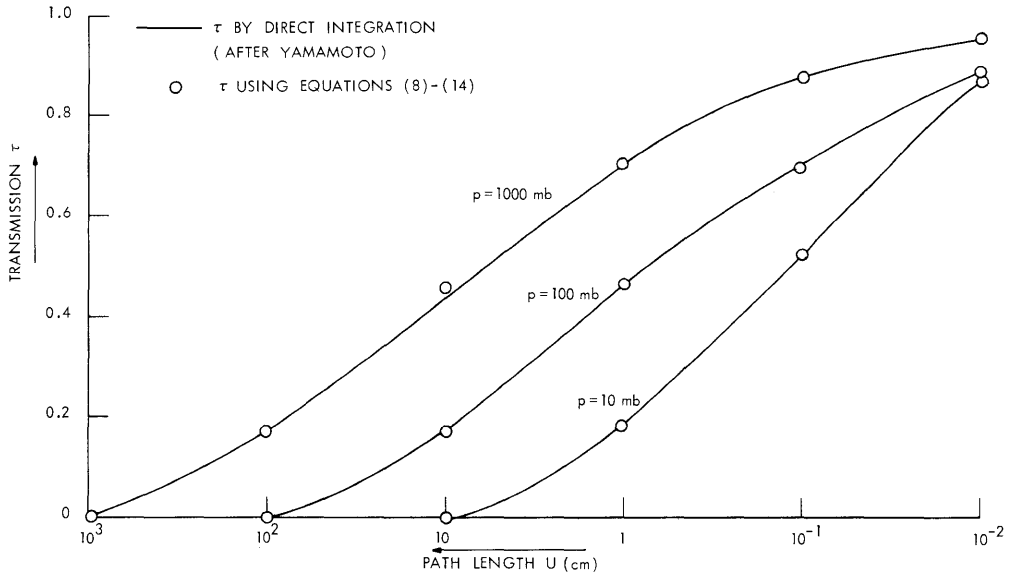

Fig. I-12. Q-branch transmission averaged over a 5 cm^{-1} channel.

and IV, where the absolute error is small instead.

Using Eqs. 8-14 and the partition scheme outlined in Fig. I-11, we evaluate the transmittance for the 667.38 cm^{-1} fundamental band of carbon dioxide (see Fig. I-12). As can be seen, the result is in excellent agreement with Yamamoto's result obtained by direct point-by-point integration using the absorption coefficient in Eq. 4 at each point.

R. K. L. Poon, D. H. Staelin

References

1. G. Yamamoto and M. Aida, "Evaluation of the Transmission of the Q Branch of the CO_2 Band," J. Quant. Spectrosc. Radiative Transfer 8, 1307 (1968).
2. NBS Applied Mathematics Series 51, "Tables of the Exponential Integral for Complex Arguments," 1958.
3. P. J. Wyatt, V. R. Stull and G. N. Plass, "Quasi-random Model of Band Absorption," J. Opt. Soc. Am. 52, 1209 (1962).